THE JOURNAL OF PHYSICAL CHEMISTRY C

pubs.acs.org/JPCC Article

Interaction of C_3–C_5 Alkenes with Zeolitic Brønsted Sites: π-Complexes, Alkoxides, and Carbenium Ions in H-FER

Qinghua Ren, Marcin Rybicki, and Joachim Sauer*

Cite This: *J. Phys. Chem. C* 2020, 124, 10067–10078 Read Online

ACCESS | Metrics & More | Article Recommendations | Supporting Information

ABSTRACT: We use a chemically accurate (4 kJ/mol) hybrid MP2:(PBE+D2) + ΔCCSD(T) method to determine relative stabilities of all possible π-complexes, alkoxides, and carbenium ions formed from propene, butene, and pentene with the Al(2)O(7) Brønsted acid site in H-FER. The energetic order is carbenium ions > *tert*-alkoxides > π-complexes as well as primary and secondary alkoxide species. Primary carbenium ions are not stationary points on the potential energy surface. The energetically most stable C3, C4, and C5 surface species are 2-propoxide, 2-butoxide, and the 2-methyl-2-butene π-complex with energies of −78, −81, and −85 kJ/mol, respectively, for formation from the corresponding alkenes. Compared to the present results, the widely applied PBE+D2 approach overbinds all species, and the energy differences are 18–24, 25–45, and 48–71 kJ/mol for π-complexes, alkoxides, and carbenium ions. Enthalpies and Gibbs free energies are calculated for 323 and 623 K within the harmonic approximation. The calculated adsorption enthalpy of *trans*-2-pentene, −93 kJ/mol, is in agreement with the experimental value, −92 kJ/mol [Schallmoser et al. *J. Am. Chem. Soc.* **2017**, *139*, 8646]. Entropy favors the more mobile species (carbenium ions, π-complexes), and the Gibbs free energy order becomes carbenium ions and *tert*-alkoxides > primary and secondary alkoxides > π-complexes.

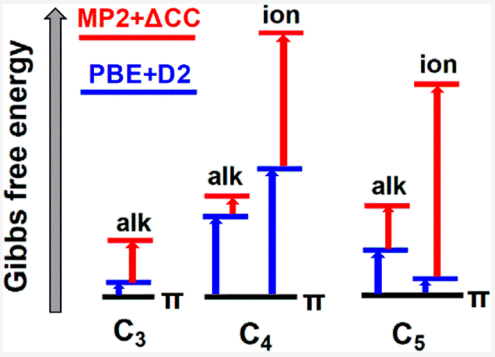

1. INTRODUCTION

Proton-exchanged zeolites play an important role in the petrochemical industry, fine chemical production, and oil refining.[1−4] Based on the acidity of their Brønsted sites, they are successfully used as catalysts for a range chemical reactions.[5−8] One application is hydrocarbon transformation reactions such as skeletal isomerization of linear alkenes. The activity of zeolites in this reaction is based on their ability to donate a proton to alkenes, forming positively charged carbenium ions as transition structures or intermediates.

Carbenium ions are supposed to play a key role in the isomerization of alkenes.[9−12] Whether protonated alkene intermediates exist as alkoxide or as carbenium ion species inside zeolites has been extensively debated in the literature.[13−15] Several experimental and computational studies suggest that small protonated alkenes do not exist in acidic zeolites in the form of free carbenium ions, but rather as alkoxides bound to the aluminosilicate framework.[9,16] According to these studies carbenium ions are transition structures, whereas alkoxides represent intermediates of the alkene isomerization reaction.[9] The recent experimental study of linear pentene over acidic H-MFI and H-FER zeolites by Schallmoser et al.[17] combines IR spectroscopy with calorimetry and provides a full description of the adsorption of light alkenes over H-MFI at 323 K. They show that in H-MFI 2-pentene dimerizes quickly, yielding a C_{10} alkoxide species. On the basis of many assumptions, the authors estimated the chemisorption enthalpy of 2-pentene to be −133 kJ/mol. With H-FER, dimerization does not occur, and calorimetric measurements are possible which yield an adsorption enthalpy of −92 kJ/mol for the π-complex of 2-pentene.

Demuth et al.[18] applied density functional theory (DFT) and investigated the skeletal isomerization of 2-pentene over acidic ZSM-22 (H-TON) and proposed that the most likely pathway involves the formation of stable secondary carbenium ions as transient intermediates. Gleeson[19] also employed DFT in a mechanistic study of the skeletal isomerization of *cis*-butene to *iso*-butene in acidic ferrierite (H-FER), which was represented by a "27T" QM cluster model consisting of 27 TO_4 tetrahedra (T = Si, Al). The results suggested that the skeletal isomerization of linear butene to form isobutene in FER might occur via a carbenium-based mechanism.

Nieminen et al.[20] used hybrid quantum mechanics:molecular mechanics (QM:MM)[21−23] to examine the stability of C_3–C_5 alkoxide species inside H-FER. Their results show that the primary and secondary alkoxide species are significantly more stable than the adsorbed alkenes and that the alkoxides become increasingly more stable with increasing carbon number.[20] The

Received: April 6, 2020
Revised: April 14, 2020
Published: April 27, 2020

https://dx.doi.org/10.1021/acs.jpcc.0c03061
J. Phys. Chem. C 2020, 124, 10067−10078

same QM:MM implementation[21−23] has been employed to examine the interaction of linear alkenes (C2−C8) with several H-zeolites. The prediction that alkoxides are significantly more stable than π-complexes, e.g., by 54−58 kJ/mol for 2-, 3-, and 4-alkenes in H-MFI,[24] needs to be revised. Below we will show that π-complexes are similarly stable as primary and secondary alkoxides.

The stability of the *tert*-butylcarbenium ion in H-FER was the focus of the computational studies of Tuma et al.[25−27] The authors investigated the potential energy surface (PES) of the isobutene/H-FER system using a multilevel hybrid QM:QM computational protocol.[26,28] This method enables estimation of the molecular energies with CCSD(T) quality. CCSD(T)—Coupled Cluster with Single and Double and Perturbative Triple substitution—is known to provide chemically accurate results.[29] The energetic order found was π−complex < alkoxides ≪ *tert*-butyl cation. Tuma et al.[25] also concluded that the widely used Perdew−Burke−Ernzerhofer (PBE) functional[30] with D2 dispersion correction[31] overestimates the relative stability of the *tert*-butyl ion by about 45 kJ/mol. This suggests that standard generalized-gradient-approximation (GGA) functionals[32,33] such as PBE, regardless of dispersion corrections, are not well-suited for studies of hydrocarbon surface species, in particular not for ionic species.

Plessow et al.[34] picked up the QM:QM methodology of Tuma and Sauer[26,28,35] and investigated alkene methylation and cracking reactions in H-SSZ-13 (H-CHA) with hybrid MP2:PBE+D3 calculations. Their results showed that the barrier for cracking depends sensitively on the involved cationic intermediates, and the *tert*-butyl cation leads to the formation of isobutene along with another alkene.

Most quantum chemical calculations on alkene reactivity over zeolites were performed by using the static approach, which takes into account only a small set of the most stable adsorption structure for each species.[36−38] However, isomerization reactions are performed at finite temperatures where an ensemble of structures may represent each species. To consider this, Cnudde et al.[39] performed molecular dynamics (MD) and metadynamics (MTD) simulations of alkene cracking intermediates (butenes and pentenes) in H-MFI on a PBE PES with D3 dispersion correction.[31] They compared their dynamic results with static calculations for the same potential energy surface. For linear alkenes, their static results show that the adsorption π-complex and the corresponding alkoxides are comparable in energy and much more stable than the carbenium ions. For the branched intermediates, tertiary carbenium ions are strongly stabilized and at 0 K are almost as stable as the π-complexes and corresponding alkoxides. At high temperature (773 K) the entropic penalty strongly destabilizes alkoxides, whereas the π-complexes are the most stable species. The MD simulations show that the shape of the free energy surface depends strongly on temperature. At 323 K the conclusions are similar to those for the static approach at low temperature. However, at the temperature of 773 K alkoxides are not stable anymore, whereas the carbenium ions of either linear or branched alkenes are entropically stabilized, in contrast to the results of the static calculations. The same conclusion has been reached many years ago for isobutene/H-FER by Tuma and Sauer,[27] who showed that with increasing temperature the entropy disfavors alkoxides relative to the π-complexes and the *tert*-butyl cation. Recently Rey et al. investigated the isomerization reactions of alkenes on acid chabazite using molecular dynamics free energy simulations.[40,41] Their results showed that the rate constant of type A isomerization involving a direct alkyl transfer is higher than that of type B isomerization involving nonclassical carbenium ions in chabazite.

The majority of computational studies on hydrocarbon reactions in acidic zeolites are performed with what may be called the "standard approach", namely, PBE+D2/D3 energy calculations for stationary points and free energies from harmonic vibrational partition functions. To get reliable results relevant for experiment, the "standard approach" needs improvement for both sampling of the PES (using MD and metadynamics)[39−41] and accurately calculating the PES using hybrid QM:QM methods.[35] Here, we focus on improving the PES, and we will show that PBE+D2/D3 overbinds all surface species significantly, but to a different extent, so that the relative stabilities of π-complexes, alkoxides, and carbenium ions are seriously affected.

Aiming for chemical accuracy (4.2 kJ/mol), in this work we perform hybrid MP2:(PBE+D2)+ΔCCSD(T) calculations[26,28,35,42−44] to determine relative stabilities of all possible intermediates of propene, butene, and pentene isomers in H-FER (proton form of ferrierite), including π-adsorption complexes, alkoxides, and carbenium ions. This method has been shown to yield chemical accuracy for energy barriers[45] and adsorption energies.[46] It has recently been applied to calculate proton exchange barriers for alkanes in H-MFI.[47] Employing a single-point version of the hybrid MP2:(PBE+D3) method, Plessow et al.[48] investigated the initiation of the methanol-to-alkene process using a multiscale modeling approach where more than 100 ab initio computed rate constants for H-CHA are used in a batch reactor model to find the dominant initiation pathway.

2. COMPUTATIONAL MODELS AND METHODS

2.1. DFT Calculations and Periodic Model. We adopted the periodic H-FER zeolite model of Tuma and Sauer,[25] with the orthorhombic unit cell of the pure silica FER framework. The structure optimization using PBE+D2[30,31] resulted in *a*, *b*, and *c* lattice constants of 19.117, 14.318, and 15.128 Å, respectively. By substitution of a silicon atom in the T2 position with aluminum and addition of a charge neutralizing proton to the oxygen in O(7) position, a unit cell with $HAlSi_{71}O_{144}$ composition (Al/Si ratio of 1/71) was obtained (see Figure 1a). The Al(2)O(7) Brønsted site was found to be energetically most stable[20] and has been adopted in previous studies.[20,25] From this H-FER structure, models were designed for all π-adsorption complexes of propene, butenes, and pentenes, all possible alkoxides formed upon the chemisorption of these alkenes, and all stable carbenium ions.

Following previous studies,[45,47] DFT calculations were performed with periodic boundary conditions at the Γ-point using the Vienna Ab Initio Package (VASP),[49,50] version 5.3.5, which used a plane-wave kinetic energy cutoff of 400 eV and the projector-augmented wave (PAW) method[51] to describe core electrons. The PBE exchange-correlation functional was applied[30] together with Grimme's D2 dispersion term[31] as implemented with periodic boundary conditions by Kerber et al.[52] The SCF energy convergence criterion was 10^{-7} eV, and structure optimizations were considered converged when the maximum force acting on the atoms was $<10^{-3}$ eV/Å. The stationary points were subsequently characterized as minima by normal-mode analysis. Harmonic vibrational energies were determined from partial Hessian matrices, which were calculated numerically by using central differences with Cartesian displace-

https://dx.doi.org/10.1021/acs.jpcc.0c03061
J. Phys. Chem. C 2020, 124, 10067−10078

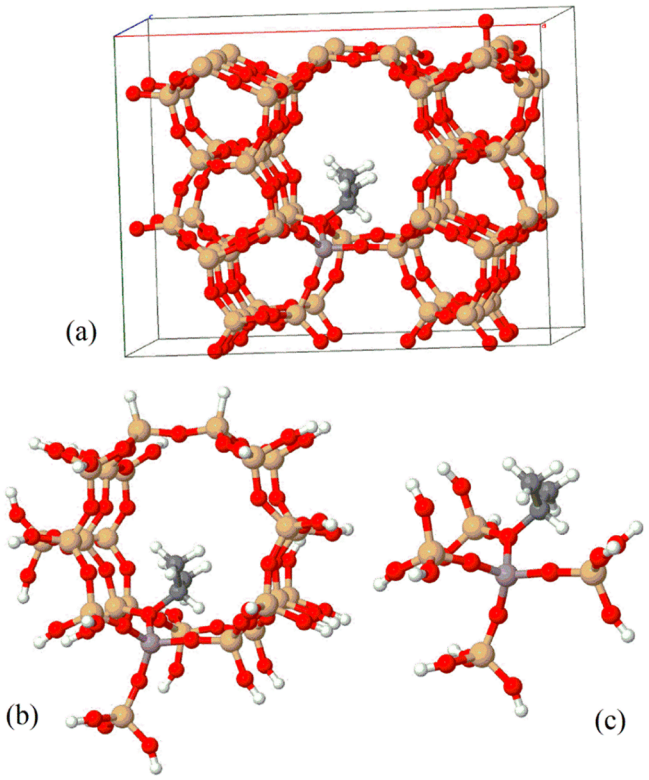

Figure 1. (a) Unit cell model for PBE+D2 calculations (fully optimized structure of 2-propoxide). (b) Large cluster model for B3LYP:PBE+D2 and MP2:PBE+D2 calculations. (c) Small (5T) cluster model for ΔCCSD(T) corrections.

ments of 0.02 Å. The partial Hessian included all atoms of the large cluster model shown in Figure 1b.

2.2. Hybrid QM:QM Calculations. We use here the mechanical embedding scheme,[21−23] which partitions the whole system (S) into an inner and an outer region. For zeolites, cutting out the inner region creates dangling bonds, which are saturated with H atoms as link atoms. The inner part and link atoms form the cluster (C). The total hybrid energy of the system, $E_{HL:LL}(S)$, is obtained as follows:[21,22]

$$E_{HL:LL}(S) = E_{HL}(C) + E_{LL}(S) - E_{LL}(C) \quad (1)$$

To the high-level energy of the cluster, $E_{HL}(C)$, the energy of the full system obtained at the low-level, $E_{LL}(S)$, is added. The third contribution, $E_{LL}(C)$, approximately eliminates the double counting of the contributions coming from atoms in the inner region and artificial contributions from link atoms. Figure 1b shows the cluster model adopted to perform high-level calculations (MP2 or B3LYP). Obtaining reliable hybrid QM:QM results needs a careful selection of the cluster model for the high-level calculations. We designed models from all alkoxides formed upon the chemisorption of these C_3−C_5 alkenes and did calculations with different model sizes. For both relative and adsorption energies, increasing the cluster size beyond the 5T model does not change the hybrid results anymore. Therefore, the larger cluster, depicted in Figure 1b, was used for all further hybrid QM:QM calculations.

Our QM:QM calculations employed the MonaLisa program.[53] The low-level calculations for the whole periodic system are performed with PBE+D2 with the same settings as described in the previous section. Low-level PBE+D2 cluster calculations were performed with ORCA program version 4.0.1[54] using def2-TZVP basis sets.[55] For π-complexes, the results were corrected for basis set superposition errors (BSSE).

Equation 1 is valid also for determining the forces which make structure optimizations at the hybrid QM:QM potential energy surface (PES) possible. Our test calculation (see Table S6 in the Supporting Information) showed that optimization of the structures at the hybrid MP2:PBE+D2 level did not change the energies more than 1 kJ/mol compared to the hybrid energies calculated at PBE+D2 optimized structures.[47] Therefore, in this work, we do not optimize the structures at the hybrid PES, but we calculate single-point hybrid MP2:PBE+D2 energies at the PBE+D2 equilibrium structures.

2.3. Wave-Function-Based Electron Correlation Methods. As the high-level method we use domain based local pair natural orbital (DLPNO) MP2[56] as implemented in the ORCA program version 4.0.1.[54] Our test calculations have shown that the DLPNO-MP2 results agree with the canonical ones within 1.3 kJ/mol (see Table S7). From hereon, we will drop the DLPNO abbreviation. MP2 energies were extrapolated to the complete basis set limit using a two-point extrapolation scheme[57,58] with cc-pV*X*Z basis sets, *X* = T, Q.[59,60] The energies used for the extrapolation were corrected for the BSSE by using the counterpoise correction (CPC) scheme.[61] To apply

Table 1. Energies, ΔE_{ads},[a] Enthalpies, ΔH_{ads},[b] and Gibbs Free Energies, ΔG_{ads},[c] of Adsorption of Alkenes at the Al(2)O(7) BAS of H-FER (in kJ/mol)

	ΔE_{ads}[a,d]				ΔH_{ads}[b,d]		ΔG_{ads}[c,d]	
alkene	PBE+D2	Δ_{HL}[e]	Δ_{CC}[f]	MP2+ΔCC	323 K	623 K	323 K	623 K
3Pi_1	−82.6	12.0	6.0	−64.6	−60.2	−56.6	−8.3	38.7
4Pi_1	−91.2	16.5	5.5	−69.2	−64.6	−60.9	−13.4	32.8
4Pi_i	−92.1	17.2	5.3	−69.6	−65.3	−61.7	−15.2	30.1
4Pi_t-2	−96.1	14.1	5.2	−76.8	−72.6	−68.8	−22.6	22.5
4Pi_c-2	−98.9	12.9	5.0	−81.0	−76.9	−73.2	−24.2	23.5
5Pi_1	−102.0	19.7	4.3	−78.0	−73.2	−69.1	−18.4	31.0
5Pi_3-M-1	−103.9	14.5	5.2	−84.2	−78.8	−75.2	−22.8	28.1
5Pi_2-M-2	−109.7	17.9	6.5	−85.3	−80.9	−77.3	−25.8	24.1
5Pi_i	−107.1	14.0	5.9	−87.2	−82.2	−78.6	−25.7	25.4
5Pi_t-2	−109.8	15.6	6.1	−88.1	−83.1[g]	−79.5	−30.3	17.5
5Pi_c-2	−114.2	15.5	6.0	−92.7	−88.6[g]	−84.9	−32.7	17.9

[a] $\Delta E_{ads} = E(\text{ads-}\pi) - E(\text{zeolite}) - E(\text{alkene})$. [b] $\Delta H_{ads} = \Delta E + (\Delta H - \Delta E)_{PBE+D2}$ (eq 6). [c] $\Delta G = \Delta H + T\Delta S_{PBE+D2}$ (eq 7). [d] Structures optimized by using PBE+D2. [e] High-level correction (eq 4). [f] CCSD(T) correction, Δ_{CC} (kJ/mol) (eq 2). [g] The experimental value is −92 kJ/mol (ref 17).

https://dx.doi.org/10.1021/acs.jpcc.0c03061
J. Phys. Chem. C 2020, 124, 10067−10078

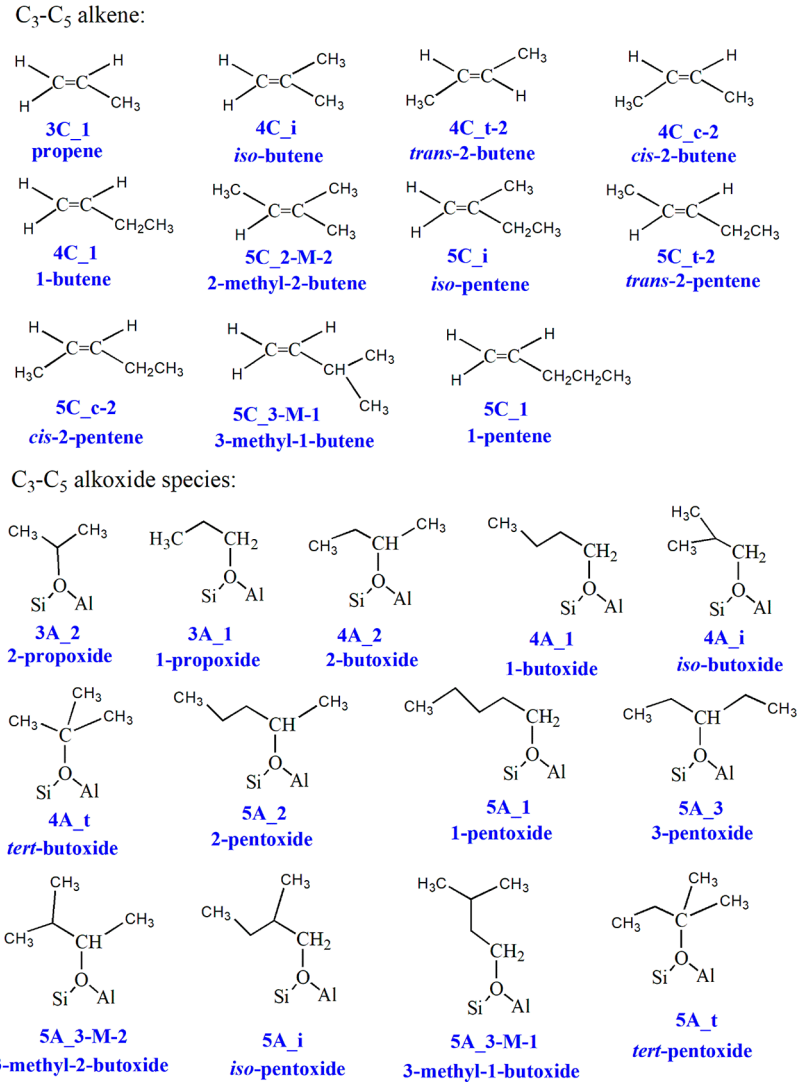

Figure 2. Structures, names, and abbreviations of investigated hydrocarbon species.

the counterpoise procedure to adsorption complexes, we split the system into the alkene molecule and the acidic zeolite part.[47,62,63] To account for higher order electron correlation effects, we performed the domain-based local pair natural orbital DLPNO-CCSD(T) method[64] for the small clusters (shown in Figure 1c) using the same extrapolation scheme as in MP2 calculations.

The difference between CCSD(T) and MP2 electron correlation contributions obtained with the small cluster models

$$\Delta_{CC}(C_{small}) = \Delta E_{CCSD(T)}(C_{small}) - \Delta E_{MP2}(C_{small}) \quad (2)$$

when added to the hybrid MP2:PBE+D2 results yields our final estimates for adsorption and reaction energies:

$$\Delta E = \Delta E_{MP2:PBE+D2} + \Delta_{CC} \quad (3)$$

It will be termed hybrid MP2:(PBE+D2) + ΔCC energy.

The so-called high-level correction, Δ_{HL}, is defined as a difference between the MP2:PBE+D2 results and the low-level energies:

$$\Delta_{HL} = \Delta E_{MP2} - \Delta E_{PBE+D2} \quad (4)$$

and provides a quality measure of the low-level method, in our case PBE+D2. For details of how to obtain the hybrid MP2:(PBE+D2) + ΔCC energies and for the summary of the computational protocol, see ref 47.

2.4. Enthalpy and Gibbs Free Energy Calculations. To compare computational results with experiments, we calculated zero-point vibrational energies, ΔE_{ZPV}, and vibrational contributions to thermal energies, ΔE_{therm}, within the harmonic approximation[65,66] at the PBE+D2 level. The enthalpy of processes of interest is calculated as

$$\Delta H = \Delta E_{el} + \Delta E_{ZPV} + \Delta E_{therm} + p\Delta V \quad (5)$$

where ΔE_{el} is the electronic energy of the process, p is the pressure, and ΔV is the change of the volume during the process. The $p\Delta V$ term is $-RT$ for formation of surface bound species. Our best final enthalpy values, ΔH (see Tables 1−4), are calculated according to eq 5 with electronic energies obtained at the hybrid QM:QM level and the remaining terms, abbreviated as $(\Delta H - \Delta E_{el})_{PBE+D2}$, calculated at the PBE+D2 level within the harmonic approximation:

$$\Delta H = \Delta E + (\Delta H - \Delta E_{el})_{PBE+D2} \quad (6)$$

Our final Gibbs free energy values at temperature T, $\Delta G(T)$, are calculated by using the final enthalpy values, eq 5, and the entropy change, ΔS.[65,66]

https://dx.doi.org/10.1021/acs.jpcc.0c03061
J. Phys. Chem. C 2020, 124, 10067−10078

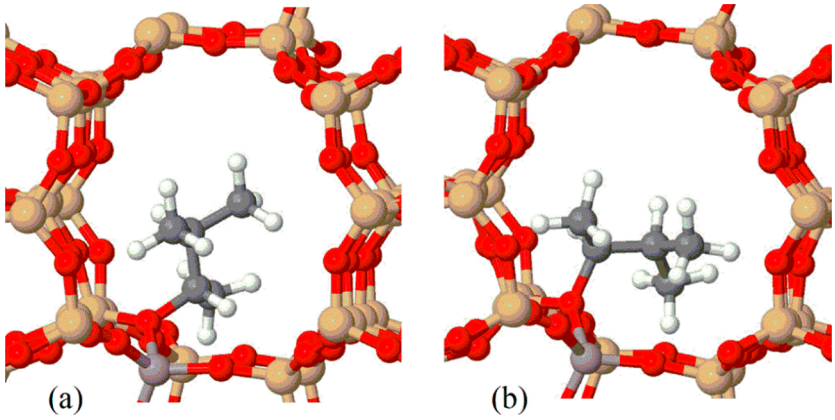

Figure 3. Optimized structures of 3-methyl-2-butoxide species (PBE+D2 calculations): (a) the lowest energy conformation; (b) the high energy (+86 kJ/mol) conformation.

$$\Delta G(T) = \Delta H - T\Delta S_{\mathrm{PBE+D2}} \quad (7)$$

3. RESULTS AND DISCUSSION

3.1. Surface Species Investigated. We investigate here all possible surface species formed on adsorption and chemisorption of all isomers of propene, butene, and pentene in H-FER at the Al(2)O(7) Brønsted acid site (BAS), namely, π-adsorption complexes, alkoxides, and carbenium ions. Figure 2 shows our nomenclature for the gas phase alkenes and the surface alkoxides. For alkenes we use *n*C_*x*-*p*, where *n* represents the number of carbon atoms in the hydrocarbon part, *p* indicates the position of the double bond, or is the conventional name of the alkene, e.g., 4C_i represents isobutene, and *x* is optional and may contain information about the conformation (c for *cis*-, t for *trans*-) or the position of an additional substituent, e.g., 4C_t-2 represents *trans*-2-butene. For π-adsorption complexes we only replace C with Pi, i.e., 4Pi_t. For alkoxide species we use *n*A_*x*-*p*, but here *p* indicates the position of the C−O bond. For carbenium ions we use the nomenclature of the alkoxide species and just replace A with I, e.g., 4I_t.

All surface species were fully optimized by using PBE+D2. Finding global minimum structures requires a very careful scanning of the conformational space of adsorbed molecules, which is particularly challenging for pentene isomers. For example, the conformation shown in Figure 3a was the lowest energy structure for 3-methyl-2-butoxide, whereas optimization of the conformation shown in Figure 3b resulted in a local minimum which was +86 kJ/mol higher in energy. In most cases, however, the energy differences were below 20 kJ/mol. We did not apply global optimization techniques, but given the large number of structures (locally) optimized, nearly 1000, there is a very high probability that the most stable isomer for each species is included.

3.2. Adsorption Energies of π-Complexes. We use three methods, PBE+D2, MP2:(PBE+D2)+ΔCC//PBE+D2 (abbrev: MP2+ΔCC), and B3LYP+D2:(PBE+D2)//PBE+D2 (abbrev: B3LYP), to study propene, butenes, and pentenes adsorbed at the Al(2)O(7) BAS of H-FER. In all these calculations, we used the structures optimized using PBE+D2. Following the Pople School, the double slash, "...//..." stands for "at the structure of". For the B3LYP results see the Supporting Information. Table 1 lists the adsorption energies for the π-complexes of propene, butenes, and pentenes of H-FER. Figure 4 shows the MP2+ΔCC adsorption energies for different C numbers. The adsorption energies were calculated as the difference between the total energy of the complex and the sum of the energies of the optimized bare zeolite and the parent alkene optimized in the gas phase.

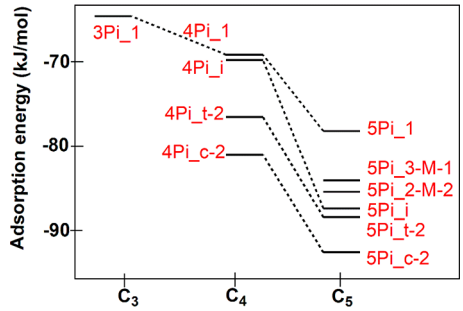

Figure 4. MP2+ΔCC adsorption energies of C_3−C_5 alkenes on the Al(2)O(7) BAS of H-FER.

As expected, the adsorption energies get more negative with increasing carbon atom number. The most negative value corresponds to *cis*-2-butene (4C_c-2) and *cis*-2-pentene (5C_c-2) for C_4 and C_5 alkenes, respectively. Decomposing the adsorption energy in contributions from the double bond, $E_{C=C}$, and from methyl substituents, E_{Me}, suggests

$$\Delta E_{ads} = E_{Me}(N_C - 2) + E_{C=C} \quad (8)$$

With the MP2+ΔCC adsorption energies we get for the 3Pi_1, 4Pi_1, and 5Pi_1 series, ΔE_{ads}= −6.7(N_C − 2) −57.2 kJ/mol (R^2 = 0.94), and for the series of the most stable π-complexes, 3Pi_1, 4Pi_c-2, and 5Pi_c-2, ΔE_{ads}= −14.0(N_C − 2) −51.2 kJ/mol (R^2 = 0.98).

The MP2+ΔCC adsorption energies are 18−24 kJ/mol less binding than the corresponding PBE+D2 results (Δ_{HL}+ Δ_{CC} in Table 1). The deviation is much larger than found for alkane adsorption on H-MFI,[47] 8−9 kJ/mol, or on H−CHA,[46] 8−13 kJ/mol. The CCSD(T) contribution (Δ_{CC}) to the deviation is about 5 kJ/mol for the alkene adsorption in H-FER (see Table 1), which indicates that the MP2 slightly overestimates the stability of π-complexes with respect to more accurate CCSD(T) method. This behavior is different from the one observed for the alkane adsorption in H-MFI, where MP2 and CCSD(T) methods give similar adsorption energies (±1 kJ/mol).[47] The QM:MM adsorption energies of Nieminen et al.[20] are about 8−30 kJ/mol less binding than our hybrid QM:QM results shown in Table 1.

https://dx.doi.org/10.1021/acs.jpcc.0c03061
J. Phys. Chem. C 2020, 124, 10067−10078

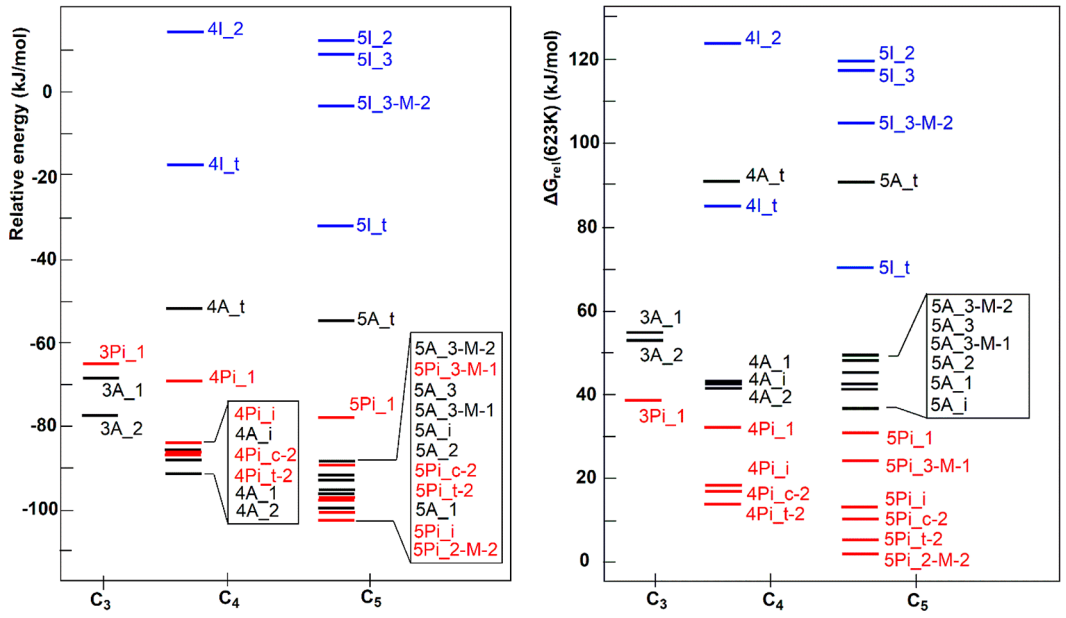

Figure 5. (a) Energies, ΔE, and (b) Gibbs free energies, ΔG(623 K), of alkoxides, π-complexes, and carbenium ions at the Al(2)O(7) BAS of H-FER relative to the respective 1-alkenes in the gas phase (kJ/mol). The energy values are reported in Table S1.

Table 2. Energies, ΔE_{rel}[a] (in kJ/mol), as Well as Enthalpies, ΔH_{rel},[b] and Gibbs Free Energies, ΔG_{rel},[c] at 323 and 623 K (in kJ/mol) of Gas Phase Alkenes Relative to the Respective 1-Alkenes

	ΔE_{rel}[a,d]				ΔH_{rel}[b,d]		ΔG_{rel}[c,d]	
alkene	PBE+D2	Δ_{HL}[e]	Δ_{CC}[f]	MP2+ΔCC	323 K	623 K	323 K	623 K
4C_i	−17.7	0.9	2.0	−14.8	−16.1	−15.6	−13.7	−11.7
4C_t-2	−13.7	2.9	0.8	−10.0	−11.0	−10.8	−9.5	−8.2
4C_c-2	−10.5	4.0	0.8	−5.7	−6.0	−5.9	−5.8	−5.6
4C_1	0.0	0.0	0.0	0.0	0.0	0.0	0.0	0.0
5C_2-M-2	−24.0	3.8	3.3	−16.9	−18.6	−17.9	−19.8	−21.3
5C_i	−16.0	0.6	2.5	−12.9	−14.0	−13.5	−12.5	−11.4
5C_t-2	−12.0	1.9	1.3	−8.8	−9.6	−9.4	−10.2	−10.9
5C_c-2	−8.1	2.8	1.4	−3.9	−3.8	−3.7	−5.6	−7.3
5C_3-M-1	−4.3	−2.9	2.1	−5.1	−6.1	−5.5	−5.0	−4.2
5C_1	0.0	0.0	0.0	0.0	0.0	0.0	0.0	0.0

[a] $\Delta E_{rel} = E$(alkene) − E(1-butene for C_4 alkene, or 1-pentene for C_5 alkene). [b] $\Delta H_{rel} = \Delta E + (\Delta H - \Delta E)_{PBE+D2}$ (eq 6). [c] $\Delta G_{rel} = \Delta H + T\Delta S_{PBE+D2}$ (eq 7). [d] Structures optimized by using PBE+D2 method. [e] High-level correction (eq 4). [f] CCSD(T) correction, Δ_{CC} (eq 2).

3.3. Stabilities of Different C_3−C_5 Species in H-FER. The relative MP2+ΔCC energies, ΔE, and Gibbs free energies, ΔG (623 K), of all the species are compared in Figures 5a and 5b, respectively. The sum of the energies of H-FER and propene, 1-butene, or 1-pentene is set as zero energy reference for all C_3, C_4, or C_5 species, respectively. The relative PBE+D2 energies are compared in Figure S1.

Table 3 summarizes the energies (kJ/mol) of alkoxide and carbenium ion formation from gas phase alkenes in H-FER. These energies are calculated as the difference between the total energy of the surface species and the sum of the energies of H-FER and the respective alkene isomer. They are directly related to the relative energies shown in Figures 5a and 5b, which are given, however, with respect to the 1-alkene in the gas phase. The relative energies of different gas phase alkene isomers which are needed to convert the two sets of data into each other are given in Table 2.

Figure S3 compares the hybrid QM:QM results of this work with those of Tuma et al.[25] for surface species that can be formed from isobutene. The energetic order is the same, except for the relative energies of the π-complexes and the primary isobutoxide. The deviation mainly originates from the different basis sets used for the ΔCCSD(T) calculations. Here, we use extrapolated cc-pVTZ, cc-pVQZ results, whereas Tuma et al.[25] employed the smaller "def-"TZVP basis set. Moreover, ref 25 did not use dispersion correction for structure optimizations.

Figure 5a shows that the secondary C_3 alkoxide 3A_2 (−78 kJ/mol) is more stable than the primary alkoxide 3A_1 (−69 kJ/mol). 3A_2 has a longer C−O bond, 154 pm, compared to 151 pm for 3A_1. Similarly, the secondary alkoxide 4A_2 (−91 kJ/mol) is more stable than the primary alkoxide 4A_1 (−88 kJ/mol). 4A_2 has a longer C−O bond, 155 pm, compared to 151 pm for 4A_1. In contrast, the primary C_5 alkoxide 5A_1 (−100 kJ/mol) is more stable than the secondary alkoxide 5A_2 (−96 kJ/mol), although 5A_2 has a longer C−O bond, 155 pm, compared to 152 pm for 5A_1. The relative energies of the same type of C_3−C_5 alkoxides (primary, secondary, etc.) become lower with increasing carbon number. For example, the relative energies for the primary alkoxides 3A_1, 4A_1, and 5A_1 are −69, −88, and −100 kJ/mol, respectively.

https://dx.doi.org/10.1021/acs.jpcc.0c03061
J. Phys. Chem. C 2020, 124, 10067−10078

Table 3. Energies, ΔE,[a] as Well as Enthalpies, ΔH,[b] and Gibbs Free Energies, ΔG,[c] at 323 and 623 K for the Formation of Alkoxides and Carbenium Ions from the Respective Alkenes in the Gas Phase (in kJ/mol)

	$\Delta E^{a,d}$			$\Delta H_{final}{}^{b,d}$		$\Delta G_{final}{}^{c,d}$	
reaction	PBE+D2	Δ^e	MP2+ΔCC	323 K	623 K	323 K	623 K
3C_1 → 3A_2	−106.6	28.6	−78.0	−67.0	−65.2	−4.1	53.9
3C_1 → 3A_1	−94.2	25.4	−68.8	−56.2	−55.1	1.9	55.7
4C_i→4A_i	−97.1	25.5	−71.6	−58.4	−57.3	0.6	55.1
4C_i→4A_t	−74.7	38.5	−36.2	−25.7	−23.2	41.1	102.4
4C_i→4I_t	−58.2	55.1	−3.1	−2.5	2.0	49.9	96.9
4C_t-2 → 4A_2	−109.4	28.5	−80.9	−68.8	−67.1	−6.8	50.3
4C_t-2 → 4I_2	−19.3	43.9	24.6	30.0	33.8	83.5	132.0
4C_c-2 → 4A_2	−112.6	27.3	−85.3	−73.8	−72.0	−10.5	47.8
4C_c-2 → 4I_2	−22.5	42.7	20.2	25.0	28.9	79.8	129.4
4C_1 → 4A_2	−123.1	32.1	−91.0	−79.8	−77.9	−16.3	42.1
4C_1 → 4A_1	−116.5	28.5	−88.0	−75.0	−74.0	−13.4	43.6
4C_1 → 4I_2	−33.0	47.6	14.6	19.0	23.1	74.0	123.7
5C_2-M-2 → 5A_3-M-2	−103.2	31.8	−71.4	−59.0	−57.2	8.6	70.8
5C_2-M-2 → 5A_t	−78.5	40.8	−37.7	−26.4	−24.0	45.7	112.0
5C_2-M-2 → 5I_t	−81.8	66.9	−14.9	−16.9	−12.7	40.0	91.5
5C_2-M-2 → 5I_3-M-2	−28.8	42.7	13.9	19.5	23.7	76.0	127.0
5C_i→5A_i	−111.1	28.3	−82.8	−69.4	−68.3	−8.2	48.4
5C_i→5A_t	−86.6	44.8	−41.8	−31.1	−28.4	38.5	102.2
5C_i→5I_t	−89.9	71.0	−18.9	−21.6	−17.2	32.7	81.7
5C_t-2 → 5A_2	−120.1	32.7	−87.4	−74.6	−73.1	−7.9	53.7
5C_t-2 → 5A_3	−115.8	33.3	−82.5	−69.7	−68.1	−2.7	59.2
5C_t-2 → 5I_3	−30.7	48.7	18.0	23.0	27.0	78.1	127.9
5C_t-2 → 5I_2	−31.2	53.0	21.8	26.2	30.3	81.1	130.6
5C_c-2 → 5A_2	−124.0	31.7	−92.3	−80.4	−78.8	−12.5	50.1
5C_c-2 → 5A_3	−119.7	32.3	−87.4	−75.5	−73.8	−7.3	55.6
5C_c-2 → 5I_3	−34.6	47.7	13.1	17.2	21.3	73.5	124.3
5C_c-2 → 5I_2	−35.1	52.0	16.9	20.4	24.7	76.4	127.0
5C_3-M-1→ 5A_3-M-1	−120.0	33.0	−87.0	−74.1	−73.2	−9.7	50.0
5C_3-M-1 → 5A_3-M-2	−123.0	39.7	−83.3	−71.5	−69.6	−6.3	53.7
5C_3-M-1 → 5I_3-M-2	−48.6	50.6	2.0	7.0	11.3	61.2	109.9
5C_1 → 5A_1	−131.1	31.4	−99.7	−86.7	−85.8	−20.1	41.7
5C_1 → 5A_2	−132.1	35.9	−96.2	−84.2	−82.5	−18.1	42.8
5C_1 → 5I_2	−43.2	56.2	13.0	16.6	20.9	70.8	119.7

[a] $\Delta E = E$(alkoxide or carbenium ion) − E(zeolite) − E(alkene). [b] $\Delta H = \Delta E + (\Delta H - \Delta E)_{PBE+D2}$ (eq 6). [c] $\Delta G = \Delta H + T\Delta S_{PBE+D2}$ (eq 7). [d] Structures optimized by using PBE+D2. [e] $\Delta = \Delta_{HL} + \Delta_{CC}$.

Figure 5a also shows that the energetic order is carbenium ions > *tert*-alkoxides > π-complexes and primary and secondary alkoxide species. For example, the secondary 4A_2 and the primary 4A_1 butoxides are more stable than the π-complexes, but the 4I_2 and 4I_t butyl ions and the 4A_t butoxide are less stable than the π-complexes. Most carbenium ions, such as 5I_2 (13 kJ/mol), 5I_3 (9 kJ/mol), and 4I_2 (15 kJ/mol), are energetically much less stable than the corresponding alkoxides. Only the *tert*-butyl (4I_t, −18 kJ/mol) and *tert*-pentyl (5I_t, −32 kJ/mol) ions are relatively stable, but also less than the corresponding alkoxide 4A_t (−51 kJ/mol) and 5A_t (−55 kJ/mol), respectively.

Table 3 shows that the secondary alkoxides 3A_2 and 4A_2 are the most stable C_3 and C_4 species, respectively; only for the C_5 species the primary alkoxide 5A_1 has a just 3.5 kJ/mol lower energy than 5A_2. The formation of 1-pentoxide (5A_1) from 1-pentene (5C_1) is the most exoenergetic, 100 kJ/mol, of all species shown in Table 3.

Table 3 also shows that the formation of carbenium ions is energetically less favorable than the formation of alkoxide species. Only the formation of the *tert*-carbenium ions 5I_t and 4I_t is exothermic. We could not localize minima for carbenium ions that correspond to nonbranched alkoxide species of 1-pentoxide, isopentoxide, 3-methyl-1-butoxide, 1-butoxide, and isobutoxide; neither could we localize minima for any C_3 carbenium ion structure. We conclude that the nonbranched carbenium ions are not local minima on the PES, i.e., not (metastable) intermediates. They may rather correspond to saddle points, i.e., transition structures, which are beyond the scope of this study.

All three applied methods, PBE+D2, B3LYP (see Table S4), and MP2+ΔCC, often yield the same relative energetic order for the reactions in Table 3, but sometimes PBE+D2 does not correctly describe the relative energies of formation of alkoxides. For example, the order of the PBE+D2 energies to form 5A_1 compared to form 5A_2 from 5C_1 is different from that predicted by MP2+ΔCC and also B3LYP.

Figure 5b shows the Gibbs free energies, ΔG_{rel} (623 K), for the surface C_3−C_5 species. Because entropy disfavors the surface-bound alkoxides compared to the more mobile π-complexes and carbenium ions,[27] the alkoxides are destabilized compared to the energy scale in Figure 5a, and the free energy order becomes carbenium ions and *tert*-alkoxides > primary and secondary alkoxides > π-complexes.

https://dx.doi.org/10.1021/acs.jpcc.0c03061
J. Phys. Chem. C 2020, 124, 10067−10078

Table 4. Energy Differences, ΔE,[a] as Well as Enthalpy, ΔH,[b] and Gibbs Free Energy Differences, ΔG,[b] at 323 and 623 K between Alkoxides and Carbenium Ions Formed at Al(2)O(7) BAS of H-FER (in kJ/mol)

	$\Delta E^{a,d}$			$\Delta H_{final}{}^{b,d}$		$\Delta G_{final}{}^{c,d}$	
difference (A-I)	PBE+D2	Δ^e	MP2+ΔCC	323 K	623 K	323 K	623 K
(4A_t) − (4I_t)	−16.5	−16.6	−33.1	−23.2	−25.2	−8.8	5.4
(4A_i) − (4I_t)	−38.9	−29.6	−68.5	−55.9	−59.3	−49.3	−41.8
(4A_2) − (4I_2)	−90.1	−15.5	−105.6	−98.8	−101.0	−90.3	−81.6
(5A_t) − (5I_t)	3.4	−26.3	−22.9	−9.5	−11.3	5.7	20.6
(5A_i) − (5I_t)	−21.2	−42.6	−63.8	−47.8	−51.2	−40.9	−33.2
(5A_3-M-2) − (5I_3-M-2)	−74.4	−11.0	−85.4	−78.5	−80.9	−67.5	−56.3
(5A_3) − (5I_3)	−85.1	−15.4	−100.5	−92.7	−95.1	−80.8	−68.7
(5A_2) − (5I_2)	−88.9	−20.3	−109.2	−100.8	−103.4	−88.9	−76.9

[a] $\Delta E = E$(alkoxide) − E(carbenium ion). [b] $\Delta H = \Delta E + (\Delta H - \Delta E)_{PBE+D2}$ (eq 6). [c] $\Delta G = \Delta H + T\Delta S_{PBE+D2}$ (eq 7). [d] Structures optimized by using PBE+D2. [e] $\Delta = \Delta_{HL} + \Delta_{CC}$; for comparison with PBE+D3 results for H-MFI zeolite obtained by Cnudde et al.[39] see Table S5.

This does not change with increasing temperature. For example, the ΔE_{rel} values of 4Pi_I, 4A_t, and 4I_t are in the order of 4Pi_I (−84 kJ/mol) < 4A_t (−51 kJ/mol) < 4I_t (−18 kJ/mol), but at 623 K the ΔG_{rel} values of 4Pi_I, 4A_t, and 4I_t are in the order of 4Pi_I (19 kJ/mol) < 4I_t (85 kJ/mol) < 4A_t (91 kJ/mol), respectively. We are aware that the harmonic approximation, which we use here, underestimates the entropies of the weakly bound species.[46] However, already with the harmonic approximation the $-T\Delta S$ term of the π-complexes is the smallest one. Therefore, its further reduction on including anharmonicity will not change the Gibbs free energy order of different species.

Table 4 shows the energy differences ΔE (kJ/mol) and Gibbs free energy ΔG (kJ/mol) between alkoxides and the corresponding carbenium ions. All alkoxide species are more stable than the corresponding carbenium ions. Only the *tert*-butyl and *tert*-pentyl ions are closer to the alkoxides with the differences of −33 and −23 kJ/mol, respectively, which is due to the steric hindrance and has been reported previously.[20,25]

4. DISCUSSION

John et al.[67] investigated the mechanisms for the dehydration of 1-butanol to butene isomers in the three medium pore-sized zeolites H-MFI, H-TON, and H-FER by PBE+D2. Their calculations showed that the 2-butoxide (4A_2) and isobutoxide (4A_i) species were stable intermediates and assumed the secondary carbenium ion to be a high-energy transition structure.[67] They also studied the effect of the zeolite framework on 1-butanol dehydration and concluded that the carbenium ion exists only as a transition structure.[68] Our PBE+D2 results (see Figure S1) also show that 2-butoxide (4A_2), 1-butoxide (4A_1), and isobutoxide (4A_i) are the energetically most stable species, whereas the secondary and tertiary carbenium ions 4I_2 and 4I_t, respectively, are high in energy. Minima for primary carbenium ions that correspond to 1-butoxide and isobutoxide could not be localized.

Stepanov et al. used NMR to study ^{13}C-label scrambling of 2-butene in H-FER and assumed that it proceeds via a carbenium ion as short-lived intermediate (NMR spectra could not be observed) or transition state and report an activation enthalpy of 88 ± 8 kJ/mol.[12] This is supported by our MP2+ΔCC calculations which yield 102 and 65 kJ/mol for the enthalpies of the 2-butyl- and *tert*-butylcarbenium ions, respectively, relative to the *trans*-2-butene π-complex (see also Figure 5a).

The C_3, C_4, and C_5 alkoxides in H-FER are energetically more stable than the carbenium ions (MP2+ΔCC results in Figure 5a, Figure S1, and Table 4). PBE+D2 yields results (Table 4) that are 11−26 kJ/mol less in favor of alkoxides which means that PBE+D2 overestimates the relative stability of carbenium ions. The differences between our hybrid MP2+ΔCC and PBE+D2 results (Δ in Table 3) are 25−45 kJ/mol for alkoxide species and 48−71 kJ/mol for carbenium ions. The energy corrections are largest for carbenium ions which reflects the strong overestimation of the stability of polar systems (here ion pairs) by GGA functionals (here PBE+D2) due to the self-interaction correction error inherent to these methods. With the admixture of Fock exchange in B3LYP, there is less self-interaction left, and the deviations from the MP2+ΔCC results (Table S1) are diminished for carbenium ions by about 10 to 40−59 kJ/mol (Table S1) while they remain about the same for the alkoxides, 22−42 kJ/mol (Table S1).

For linear pentenes, comparison can be made with the calorimetric measurement of Schallmoser et al.,[17] who report −92 kJ/mol (at 323 K) for the enthalpy of the π-complex of 2-butene relative to the enthalpy of 1-pentene in the gas phase. With our MP2+ΔCC calculations we obtain −92.6 and −92.4 kJ/mol for *trans*- and *cis*-2-butene, respectively, in perfect agreement with experiment.

Schallmoser et al.[17] also measured the reaction heat for the dimerization of 2-pentene in H-MFI (−285.7 kJ/mol, calorimetry). They observed that the broad IR band around 3100 cm^{-1} that is characteristic of the H-bond between the OH group of the BAS and the π-bond of the alkene disappears in the course of the reaction and concluded that a C_{10} alkoxide was formed. Assuming 88 kJ/mol for the gas phase dimerization, they arrived at an estimate of −197 kJ/mol for the heat of the C10-alkoxide on the surface relative to the gas phase. This was 41 kJ/mol more exothermic than their estimate for formation of the corresponding π-complex, −156 kJ/mol (120 kJ/mol for dispersion forces and 36 kJ/mol for the π-BAS interaction). As support for the significantly more negative enthalpy of the alkoxide, they cite previous hybrid QM:MM calculations of Nguyen et al.,[24] who found alkoxides 54−58 kJ/mol more stable than the corresponding π-complexes. However, support from quantum chemistry fades away with the present QM:QM calculations. Our MP2+ΔCC enthalpies predict 2-pentoxide to be slightly less stable (−75 kJ/mol, Table 3) than the 2-pentene π-complex (−83 kJ/mol, Table 1). Adding 5 × −12 = −60 kJ/mol for the interaction of the pentyl group with the silica wall,[17,69] we arrive at estimates of −135 and −143 kJ/mol for formation of a C_{10} alkoxide and a decene π-complex, respectively. While the latter is close to the estimate of Schallmoser et al.[17] (−156 kJ/mol), our estimate for the alkoxide is 62 kJ/mol less binding than theirs (−197 kJ/mol),

https://dx.doi.org/10.1021/acs.jpcc.0c03061
J. Phys. Chem. C 2020, 124, 10067−10078

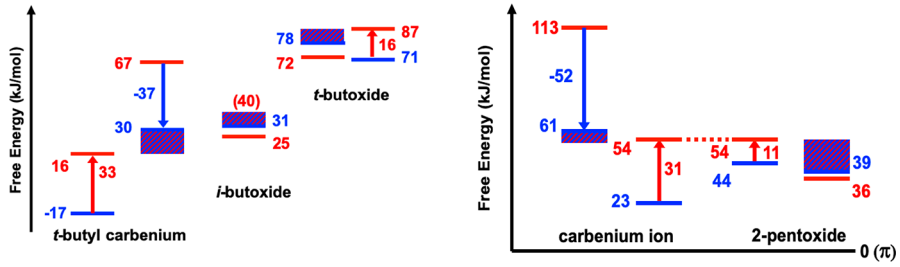

Figure 6. Comparison of metadynamics and "static" PBE+D3 free energies of alkoxide and carbenium ion species relative to π-complexes from Cnudde et al.[39] for H-MFI (773 K) with "static" MP2+ΔCC results for H-FER (623 K) from this work.

which suggests that dimerization of alkenes in H-MFI is not yet fully understood.

Cnudde et al.[39] studied the nature of adsorbed C_4 and C_5 alkene intermediates in H-MFI not only at 323 K but also at typical alkene cracking temperatures (773 K) using PBE+D3. In the following discussion we will assume that their results for H-MFI are directly comparable with our results for H-FER, an assumption that has been also made by Schallmoser et al.[17] in their study of adsorption and surface reactions of pentenes. Compared to our PBE+D2 adsorption (π-complex formation) energies (Table 1) for isobutene, *trans*-2-butene, and *trans*-2-pentene (Table 1), their PBE+D3 results (Table 1 of ref 39) are 11 kJ/mol more binding. For *trans*-2-pentene, this increases the deviation of ΔH_{ads}(323 K) from experiment (−92 kJ/mol)[17] from −13 kJ/mol (PBE+D2, Table 1, this work) to −23 kJ/mol (PBE+D3, ref 39).

The ΔE results of Cnudde et al.[39] show that the tertiary carbenium ion (4I_t) is less stable than the tertiary alkoxide (4A_t), but the ΔG results for 323 and 773 K show that with increasing temperature the alkoxide (4A_t) becomes increasingly less stable than the carbenium ion (4I_t), which is in line with our results in Figure 5. Table S5 shows the comparison between this work with PBE+D2 for H-FER and the PBE+D3 results for H-MFI,[39] which are up to 10 kJ/mol more favorable for the carbenium ions. Furthermore, in agreement with ΔG(623 K) results of this work, the ΔG(773 K) results for H-MFI show preference for the carbenium ion only for the *tert*-butyl and *tert*-pentyl species.

Free energy calculations for molecule−surface interactions in general and for adsorption and reactions in zeolite catalysts in particular have to meet two challenges: the accuracy of the PES and the sampling of the PES. The "static" approach, PBE+D2/D3 energy calculations for stationary points and free energies from vibrational partition functions, needs improvement in two directions. Aiming at chemical accuracy (4.2 kJ/mol), in this work, we focus on the improvement of the PES using hybrid MP2:(PBE+D2)+ΔCC//PBE+D2 calculations for stationary points, while for high temperatures (773 K) Cnudde et al.[39] go beyond the "static" approach and use molecular dynamics and metadynamics to sample the PES.

Figure 6 compares the free energies of alkoxides and carbenium ions relative to the π-complexes obtained by Cnudde et al.[39] with metadynamics for the PBE+D3 PES (blue lines and numbers, see Figure 7 of ref 39) with the "static" MP2+ΔCC results from this work (red lines and numbers). We approach the best estimate in two ways. We add the difference between the MP2+ΔCC energies and the PBE+D2 energies ($\Delta = \Delta_{HL} + \Delta_{CC}$ in Tables 1 and 3, red arrows) from this study to the metadynamics results, and in turn we add the difference between the metadynamic and "static" results (blue arrows, see Figure 7 of ref 39) to our MP2+ΔCC results.

With the MP2+ΔCC energy increment of 33 kJ/mol, the *tert*-butyl ion becomes 16 kJ/mol less stable than the π-complex, and with the decrement of 37 kJ/mol for passing from the static to the metadynamic result the MP2+ΔCC result changes from 67 to 30 kJ/mol. We conclude that the stability of the carbenium ion relative to the π-complex is between 16 and 30 kJ/mol (blue-red shaded area in Figure 6); i.e., the π-complex is the most stable species also at high temperature. For the *tert*-butoxide the MP2+ΔCC increment is only half of that for the carbenium ion (16 kJ/mol), and metadynamics shifts the free energy 6 kJ/mol upward. Hence, the estimated stability relative to the π-complex is between 78 and 87 kJ/mol. That the *tert*-butoxide is much less stable than the corresponding carbenium ion has been known for a long time[25−27] and mainly due to the steric repulsion which is much reduced in the isobutoxide. If we apply the same changes as calculated for *tert*-butoxide, the estimated relative stability of isobutoxide is between 25 and 40 kJ/mol, not much higher than the range of 16−30 kJ/mol for the *tert*-carbenium ion.

For 2-pentene (Figure 6, right), PBE+D3 metadynamics finds the 2-pentyl cation 44 − 23 = 21 kJ/mol more stable than 2-pentoxide (ref 39, Figure 7, left). After our MP2+ΔCC energy correction is applied, both species are predicted to be 54 kJ/mol less stable than the π-complex of 2-pentene. On the other hand, starting with the "static" MP2+ΔCC results, we arrive at 61 and 39 kJ/mol for the 2-pentyl cation and the 2-pentoxide, respectively. The estimated range of free energies relative to the π-complex is thus 54−61 kJ/mol for the carbenium ion and 39−54 kJ/mol for the 2-pentoxide, suggesting that the two species may be about equally stable with a slight preference for the 2-pentoxide.

For both the butyl and the pentyl species, we see that the MP2+ΔCC correction destabilizes the carbenium ion with respect to the π-complex (by 31−33 kJ/mol) and also with respect to the alkoxide (by 17−20 kJ/mol), which reflects the overstabilization of polar structures by PBE+D2/D3 due to the self-interaction correction error. In contrast, passing from the "static" to the metadynamic approach significantly stabilizes, by 37−52 kJ/mol, the carbenium ion with respect to both the π-complex and the alkoxide.

5. CONCLUSION

Our chemically accurate hybrid MP2:PBE+D2 + ΔCCSD(T) results show that primary and secondary alkoxides are the energetically most stable surface species in H-FER. The corresponding π-adsorption complexes are very similar in energy. The nonbranched carbenium ions are not stationary points on the potential energy surface, whereas tertiary carbenium ions (butyl and pentyl) are metastable species

https://dx.doi.org/10.1021/acs.jpcc.0c03061
J. Phys. Chem. C 2020, 124, 10067−10078

(minima on the potential energy surface). The energetic order is carbenium ions > *tert*-alkoxides > π-complexes as well as primary and secondary alkoxide species.

Because entropy disfavors the surface-bound alkoxides compared to the more mobile π-complexes and carbenium ions, the alkoxides are destabilized, and the Gibbs free energy order becomes carbenium ions and *tert*-alkoxides > primary and secondary alkoxides > π-complexes. For high temperatures (623/723 K), compared to our "static" approach, the metadynamics simulations of Cnudde et al.[39] suggest a substantial stabilization (40−50 kJ/mol) of the carbenium ion relative to both the π-complex and the alkoxide. Taking both MP2+ΔCC energies and dynamics beyond the static approach into account, π-complexes remain the most stable species, and carbenium ions and alkoxides become comparable in stability.

Compared to our hybrid MP2:PBE+D2 + ΔCCSD(T) results, the widely applied PBE+D2 method overbinds all surface species, but to a different extent reflecting the different self-interaction correction error: 18−24 kJ/mol for the π-complexes, 25−45 kJ/mol for alkoxides, and 48−71 kJ/mol for carbenium ions. Thus, PBE+D2 (and also PBE+D3) will overstabilize carbenium ions relative to alkoxides by 10−20 kJ/mol and relative to π-complexes by 25−50 kJ/mol.

■ ASSOCIATED CONTENT

Supporting Information

The Supporting Information is available free of charge at https://pubs.acs.org/doi/10.1021/acs.jpcc.0c03061.

Relative energies, enthalpies, and Gibbs free energies obtained with PBE+D2, MP2+ΔCC, and B3LYP calculations; total energies of all species (PDF)

Molecular structures of the stationary points (POSCAR files) (ZIP)

■ AUTHOR INFORMATION

Corresponding Author

Joachim Sauer − *Institute of Chemistry, Humboldt-Universität zu Berlin, 10099 Berlin, Germany;* orcid.org/0000-0001-6798-6212; Email: js@chemie.hu-berlin.de

Authors

Qinghua Ren − *Department of Chemistry, Shanghai University, Shanghai 200444, China;* orcid.org/0000-0001-8565-9653

Marcin Rybicki − *Institute of Chemistry, Humboldt-Universität zu Berlin, 10099 Berlin, Germany*

Complete contact information is available at: https://pubs.acs.org/10.1021/acs.jpcc.0c03061

Notes

The authors declare no competing financial interest.

■ ACKNOWLEDGMENTS

This work has been supported by "Deutsche Forschungsgemeinschaft" (German Research Foundation) and the "Fonds der Chemischen Industrie". The calculations have been performed on the compute servers of the Quantum Chemistry Group at Humboldt University of Berlin. Q.R. was supported by China Scholarship Council (201806895022), the Natural Science Foundation of Shanghai (18ZR1414000), and the high performance computing center of Shanghai University.

■ REFERENCES

(1) Busca, G. Acid catalysts in industrial hydrocarbon chemistry. *Chem. Rev.* **2007**, *107*, 5366−5410.

(2) Kangas, M.; Kumar, N.; Harlin, E.; Salmi, T.; Murzin, D. Y. Skeletal Isomerization of Butene in Fixed Beds. 1. Experimental Investigation and Structure−Performance Effects. *Ind. Eng. Chem. Res.* **2008**, *47*, 5402−5412.

(3) Primo, A.; Garcia, H. Zeolites as catalysts in oil refining. *Chem. Soc. Rev.* **2014**, *43*, 7548−7561.

(4) Serrano, D. P.; García, R. A.; Vicente, G.; Linares, M.; Procházková, D.; Čejka, J. Acidic and catalytic properties of hierarchical zeolites and hybrid ordered mesoporous materials assembled from MFI protozeolitic units. *J. Catal.* **2011**, *279*, 366−380.

(5) Corma, A. Inorganic Solid Acids and Their Use in Acid-Catalyzed Hydrocarbon Reactions. *Chem. Rev.* **1995**, *95*, 559−614.

(6) Perego, C.; Ingallina, P. Recent advances in the industrial alkylation of aromatics: new catalysts and new processes. *Catal. Today* **2002**, *73*, 3−22.

(7) Maihom, T.; Pantu, P.; Tachakritikul, C.; Probst, M.; Limtrakul, J. Effect of the Zeolite Nanocavity on the Reaction Mechanism of n-Hexane Cracking: A Density Functional Theory Study. *J. Phys. Chem. C* **2010**, *114*, 7850−7856.

(8) Al-Khattaf, S.; Ali, S. A.; Aitani, A. M.; Žilková, N.; Kubička, D.; Čejka, J. Recent Advances in Reactions of Alkylbenzenes Over Novel Zeolites: The Effects of Zeolite Structure and Morphology. *Catal. Rev.: Sci. Eng.* **2014**, *56*, 333−402.

(9) Kazansky, V. B. Adsorbed carbocations as transition states in heterogeneous acid catalyzed transformations of hydrocarbons. *Catal. Today* **1999**, *51*, 419−434.

(10) de Ménorval, B.; Ayrault, P.; Gnep, N. S.; Guisnet, M. Mechanism of n-butene skeletal isomerization over HFER zeolites: a new proposal. *J. Catal.* **2005**, *230*, 38−51.

(11) de Ménorval, B.; Ayrault, P.; Gnep, N. S.; Guisnet, M. n-Butene skeletal isomerization over HFER zeolites: Influence of Si/Al ratio and of carbonaceous deposits. *Appl. Catal., A* **2006**, *304*, 1−13.

(12) Stepanov, A. G.; Arzumanov, S. S.; Luzgin, M. V.; Ernst, H.; Freude, D. In situ monitoring of n-butene conversion on H-ferrierite by 1H, 2H, and 13C MAS NMR: kinetics of a double-bond-shift reaction, hydrogen exchange, and the 13C-label scrambling. *J. Catal.* **2005**, *229*, 243−251.

(13) Boronat, M.; Viruela, P.; Corma, A. The skeletal isomerization of but-1-ene catalyzed by theta-1 zeolite. *Phys. Chem. Chem. Phys.* **2001**, *3*, 3235−3239.

(14) Nicholas, J. B.; Haw, J. F. The Prediction of Persistent Carbenium Ions in Zeolites. *J. Am. Chem. Soc.* **1998**, *120*, 11804−11805.

(15) Rozanska, X.; van Santen, R. A.; Demuth, T.; Hutschka, F.; Hafner, J. A Periodic DFT Study of Isobutene Chemisorption in Proton-Exchanged Zeolites: Dependence of Reactivity on the Zeolite Framework Structure. *J. Phys. Chem. B* **2003**, *107*, 1309−1315.

(16) Haw, J. F.; Nicholas, J. B.; Xu, T.; Beck, L. W.; Ferguson, D. B. Physical Organic Chemistry of Solid Acids: Lessons from in Situ NMR and Theoretical Chemistry. *Acc. Chem. Res.* **1996**, *29*, 259−267.

(17) Schallmoser, S.; Haller, G. L.; Sanchez-Sanchez, M.; Lercher, J. A. Role of Spatial Constraints of Brønsted Acid Sites for Adsorption and Surface Reactions of Linear Pentenes. *J. Am. Chem. Soc.* **2017**, *139*, 8646−8652.

(18) Demuth, T.; Rozanska, X.; Benco, L.; Hafner, J.; van Santen, R. A.; Toulhoat, H. Catalytic isomerization of 2-pentene in H-ZSM-22—A DFT investigation. *J. Catal.* **2003**, *214*, 68−77.

(19) Gleeson, D. Skeletal Isomerization of Butene in Ferrierite: Assessing the Energetic and Structural Differences between Carbenium and Alkoxide Based Pathways. *J. Phys. Chem. A* **2011**, *115*, 14629−14636.

(20) Nieminen, V.; Sierka, M.; Murzin, D. Y.; Sauer, J. Stabilities of C3−C5 alkoxide species inside H-FER zeolite: a hybrid QM/MM study. *J. Catal.* **2005**, *231*, 393−404.

(21) Eichler, U.; Kölmel, C. M.; Sauer, J. Combining ab initio techniques with analytical potential functions for structure predictions

of large systems: Method and application to crystalline silica polymorphs. *J. Comput. Chem.* **1997**, *18*, 463−477.
(22) Sierka, M.; Sauer, J. Finding transition structures in extended systems: A strategy based on a combined quantum mechanics−empirical valence bond approach. *J. Chem. Phys.* **2000**, *112*, 6983−6996.
(23) Sauer, J.; Sierka, M. Combining quantum mechanics and interatomic potential functions in ab initio studies of extended systems. *J. Comput. Chem.* **2000**, *21*, 1470−1493.
(24) Nguyen, C. M.; De Moor, B. A.; Reyniers, M.-F.; Marin, G. B. Physisorption and Chemisorption of Linear Alkenes in Zeolites: A Combined QM-Pot(MP2//B3LYP:GULP)−Statistical Thermodynamics Study. *J. Phys. Chem. C* **2011**, *115*, 23831−23847.
(25) Tuma, C.; Kerber, T.; Sauer, J. The tert-Butyl Cation in H-Zeolites: Deprotonation to Isobutene and Conversion into Surface Alkoxides. *Angew. Chem., Int. Ed.* **2010**, *49*, 4678−4680.
(26) Tuma, C.; Sauer, J. Treating dispersion effects in extended systems by hybrid MP2:DFT calculations—protonation of isobutene in zeolite ferrierite. *Phys. Chem. Chem. Phys.* **2006**, *8*, 3955−3965.
(27) Tuma, C.; Sauer, J. Protonated Isobutene in Zeolites: tert-Butyl Cation or Alkoxide? *Angew. Chem., Int. Ed.* **2005**, *44*, 4769−4771.
(28) Tuma, C.; Sauer, J. A hybrid MP2/planewave-DFT scheme for large chemical systems: proton jumps in zeolites. *Chem. Phys. Lett.* **2004**, *387*, 388−394.
(29) Jensen, F. *Introduction to Computational Chemistry*; Wiley: Chicester, 1999.
(30) Perdew, J. P.; Burke, K.; Ernzerhof, M. Generalized Gradient Approximation Made Simple. *Phys. Rev. Lett.* **1996**, *77*, 3865−3868.
(31) Grimme, S. Semiempirical GGA-type density functional constructed with a long-range dispersion correction. *J. Comput. Chem.* **2006**, *27*, 1787−1799.
(32) Perdew, J. P.; Chevary, J. A.; Vosko, S. H.; Jackson, K. A.; Pederson, M. R.; Singh, D. J.; Fiolhais, C. Atoms, molecules, solids, and surfaces: Applications of the generalized gradient approximation for exchange and correlation. *Phys. Rev. B: Condens. Matter Mater. Phys.* **1992**, *46*, 6671−6687.
(33) Becke, A. D. Density-functional exchange-energy approximation with correct asymptotic behavior. *Phys. Rev. A: At., Mol., Opt. Phys.* **1988**, *38*, 3098−3100.
(34) Plessow, P. N.; Smith, A.; Tischer, S.; Studt, F. Identification of the Reaction Sequence of the MTO Initiation Mechanism Using Ab Initio-Based Kinetics. *J. Am. Chem. Soc.* **2019**, *141*, 5908−5915.
(35) Sauer, J. Ab Initio Calculations for Molecule−Surface Interactions with Chemical Accuracy. *Acc. Chem. Res.* **2019**, *52*, 3502−3510.
(36) Boronat, M.; Viruela, P.; Corma, A. Theoretical Study of the Mechanism of Zeolite-Catalyzed Isomerization Reactions of Linear Butenes. *J. Phys. Chem. A* **1998**, *102*, 982−989.
(37) Jeffrey Hay, P.; Redondo, A.; Guo, Y. Theoretical studies of pentene cracking on zeolites: C−C β-scission processes. *Catal. Today* **1999**, *50*, 517−523.
(38) Rigby, A. M.; Frash, M. V. Ab initio calculations on the mechanisms of hydrocarbon conversion in zeolites: Skeletal isomerisation and olefin chemisorption. *J. Mol. Catal. A: Chem.* **1997**, *126*, 61−72.
(39) Cnudde, P.; De Wispelaere, K.; Van der Mynsbrugge, J.; Waroquier, M.; Van Speybroeck, V. Effect of temperature and branching on the nature and stability of alkene cracking intermediates in H-ZSM-5. *J. Catal.* **2017**, *345*, 53−69.
(40) Rey, J.; Gomez, A.; Raybaud, P.; Chizallet, C.; Bučko, T. On the origin of the difference between type A and type B skeletal isomerization of alkenes catalyzed by zeolites: The crucial input of ab initio molecular dynamics. *J. Catal.* **2019**, *373*, 361−373.
(41) Rey, J.; Raybaud, P.; Chizallet, C.; Bučko, T. Competition of Secondary versus Tertiary Carbenium Routes for the Type B Isomerization of Alkenes over Acid Zeolites Quantified by Ab Initio Molecular Dynamics Simulations. *ACS Catal.* **2019**, *9*, 9813−9828.
(42) Tosoni, S.; Sauer, J. Accurate quantum chemical energies for the interaction of hydrocarbons with oxide surfaces: CH4/MgO(001). *Phys. Chem. Chem. Phys.* **2010**, *12*, 14330−14340.
(43) Boese, A. D.; Sauer, J. Accurate adsorption energies of small molecules on oxide surfaces: CO−MgO(001). *Phys. Chem. Chem. Phys.* **2013**, *15*, 16481−16493.
(44) Alessio, M.; Bischoff, F. A.; Sauer, J. Chemically accurate adsorption energies for methane and ethane monolayers on the MgO(001) surface. *Phys. Chem. Chem. Phys.* **2018**, *20*, 9760−9769.
(45) Piccini, G.; Alessio, M.; Sauer, J. Ab Initio Calculation of Rate Constants for Molecule−Surface Reactions with Chemical Accuracy. *Angew. Chem., Int. Ed.* **2016**, *55*, 5235−5237.
(46) Piccini, G.; Alessio, M.; Sauer, J.; Zhi, Y.; Liu, Y.; Kolvenbach, R.; Jentys, A.; Lercher, J. A. Accurate Adsorption Thermodynamics of Small Alkanes in Zeolites. Ab initio Theory and Experiment for H-Chabazite. *J. Phys. Chem. C* **2015**, *119*, 6128−6137.
(47) Rybicki, M.; Sauer, J. Ab Initio Prediction of Proton Exchange Barriers for Alkanes at Brønsted Sites of Zeolite H-MFI. *J. Am. Chem. Soc.* **2018**, *140*, 18151−18161.
(48) Plessow, P. N.; Studt, F. Olefin methylation and cracking reactions in H-SSZ-13 investigated with ab initio and DFT calculations. *Catal. Sci. Technol.* **2018**, *8*, 4420−4429.
(49) Kresse, G.; Furthmüller, J. Efficiency of ab-initio total energy calculations for metals and semiconductors using a plane-wave basis set. *Comput. Mater. Sci.* **1996**, *6*, 15−50.
(50) Kresse, G.; Furthmüller, J. Efficient iterative schemes for ab initio total-energy calculations using a plane-wave basis set. *Phys. Rev. B: Condens. Matter Mater. Phys.* **1996**, *54*, 11169−11186.
(51) Kresse, G.; Joubert, D. From ultrasoft pseudopotentials to the projector augmented-wave method. *Phys. Rev. B: Condens. Matter Mater. Phys.* **1999**, *59*, 1758−1775.
(52) Kerber, T.; Sierka, M.; Sauer, J. Application of semiempirical long-range dispersion corrections to periodic systems in density functional theory. *J. Comput. Chem.* **2008**, *29*, 2088−2097.
(53) Bischoff, F.; Alessio, M.; Berger, F.; John, M.; Rybicki, M.; Sauer, J. Multi-Level Energy Landscapes: The MonaLisa Program, https://www.chemie.hu-berlin.de/de/forschung/quantenchemie/monalisa, Humboldt-University, Berlin, 2019.
(54) Neese, F. Software update: the ORCA program system, version 4.0. *WIREs: Comput. Mol. Sci.* **2018**, *8*, No. e1327.
(55) Weigend, F.; Ahlrichs, R. Balanced basis sets of split valence, triple zeta valence and quadruple zeta valence quality for H to Rn: Design and assessment of accuracy. *Phys. Chem. Chem. Phys.* **2005**, *7*, 3297−3305.
(56) Pinski, P.; Neese, F. Communication: Exact analytical derivatives for the domain-based local pair natural orbital MP2 method (DLPNO-MP2). *J. Chem. Phys.* **2018**, *148*, 031101.
(57) Jensen, F. Estimating the Hartree—Fock limit from finite basis set calculations. *Theor. Chem. Acc.* **2005**, *113*, 267−273.
(58) Helgaker, T.; Klopper, W.; Koch, H.; Noga, J. Basis-set convergence of correlated calculations on water. *J. Chem. Phys.* **1997**, *106*, 9639−9646.
(59) Dunning, T. H. Gaussian basis sets for use in correlated molecular calculations. I. The atoms boron through neon and hydrogen. *J. Chem. Phys.* **1989**, *90*, 1007−1023.
(60) Woon, D. E.; Dunning, T. H. Gaussian basis sets for use in correlated molecular calculations. III. The atoms aluminum through argon. *J. Chem. Phys.* **1993**, *98*, 1358−1371.
(61) Boys, S. F.; Bernardi, F. The calculation of small molecular interactions by the differences of separate total energies. Some procedures with reduced errors. *Mol. Phys.* **1970**, *19*, 553−566.
(62) Svelle, S.; Tuma, C.; Rozanska, X.; Kerber, T.; Sauer, J. Quantum Chemical Modeling of Zeolite-Catalyzed Methylation Reactions: Toward Chemical Accuracy for Barriers. *J. Am. Chem. Soc.* **2009**, *131*, 816−825.
(63) Tuma, C.; Sauer, J. Quantum chemical ab initio prediction of proton exchange barriers between CH4 and different H-zeolites. *J. Chem. Phys.* **2015**, *143*, 102810.

https://dx.doi.org/10.1021/acs.jpcc.0c03061
J. Phys. Chem. C 2020, 124, 10067−10078

(64) Riplinger, C.; Neese, F. An efficient and near linear scaling pair natural orbital based local coupled cluster method. *J. Chem. Phys.* **2013**, *138*, 034106.
(65) Cramer, C. J. *Essentials of Computational Chemistry: Theories and Models*; Wiley: Chicester, 2002.
(66) Hobza, P.; Sauer, J.; Morgeneyer, C.; Hurych, J.; Zahradnik, R. Bonding ability of surface sites on silica and their effect on hydrogen bonds. A quantum-chemical and statistical thermodynamic treatment. *J. Phys. Chem.* **1981**, *85*, 4061−4067.
(67) John, M.; Alexopoulos, K.; Reyniers, M.-F.; Marin, G. B. Effect of zeolite confinement on the conversion of 1-butanol to butene isomers: mechanistic insights from DFT based microkinetic modelling. *Catal. Sci. Technol.* **2017**, *7*, 2978−2997.
(68) John, M.; Alexopoulos, K.; Reyniers, M.-F.; Marin, G. B. First-Principles Kinetic Study on the Effect of the Zeolite Framework on 1-Butanol Dehydration. *ACS Catal.* **2016**, *6*, 4081−4094.
(69) Sauer, J. Acidic catalysis by zeolites and the active site concept. In *On Catalysis*; Reschetilowski, W., Hönle, W., Eds.; VWB - Verlag für Wissenschaft und Bildung: Berlin, 2010; pp 136−161.

https://dx.doi.org/10.1021/acs.jpcc.0c03061
J. Phys. Chem. C 2020, 124, 10067−10078